

Effect of Yb addition on the superconducting properties of (Bi,Pb)-2212 superconductor

A. Biju, R.P. Aloysius, U. Syamaprasad *

Regional Research Laboratory (CSIR), Trivandrum 695 019, India

Received 14 June 2005; received in revised form 14 March 2006; accepted 22 March 2006

Abstract

The effects of Yb addition on the phase evolution and superconducting properties of (Bi,Pb)-2212 superconductor prepared by solid state synthesis in the polycrystalline form were studied. Yb content of the samples was varied ($x = 0-0.5$) on a general stoichiometry of $\text{Bi}_{1.7}\text{Pb}_{0.4}\text{Sr}_{2.0}\text{Ca}_{1.1}\text{Cu}_{2.1}\text{Yb}_x\text{O}_y$. Phase analysis by XRD, microstructural examination by SEM, measurements of density and superconducting properties were done to evaluate the relative performance of the samples. A Yb containing secondary phase could be distinguished from XRD analysis from $\text{Yb} > 0.3$ in the stoichiometric level. Microstructural examination showed clear and distinct morphological variation with Yb stoichiometry and a secondary phase with round edged grains was observed in the microstructure of Yb added samples. The critical current density (J_C) and superconducting transition temperature (T_C) of all the Yb added samples were found to be higher than that of the pure sample. A maximum $T_{C\text{-onset}}$ of 94.5 K and a maximum J_C 688 A/cm² has been observed for the sample with $\text{Yb} = 0.2$ in the stoichiometric level. Above this level T_C and J_C began to reduce, may be due to secondary phase formation.

© 2006 Elsevier B.V. All rights reserved.

PACS: 74.72.Hs

Keywords: (Bi,Pb)-2212 superconductor; Yb addition; Critical current density (J_C); Critical temperature (T_C)

1. Introduction

The critical transition temperature (T_C) and the critical current density (J_C) are the most important superconducting properties that would be taken into account in technological applications. Bi-based high T_C superconductors are used in fabrication of wires and tapes because of their high J_C as well as T_C . Intense studies were made in order to improve the superconducting properties of Bi-based superconductors. Among the three well known phases in the Bi-based superconductors with general formula $\text{Bi}_2\text{Sr}_2\text{Ca}_{n-1}\text{Cu}_n\text{O}_y$, where $n = 1, 2,$ and 3 (Bi-2201, Bi-2212, Bi-2223), Bi-2212 holds some advantage, firstly because

its oxygen stoichiometry is relatively invariant with respect to cationic dopings when the samples are prepared in identical conditions [1,2], secondly, it has lesser weak link problems compared with Bi-2223.

Among the efforts that have been made to improve the superconducting properties of Bi-2212, the substitution of Bi by Pb gives promising results [3–8] and the substitution of rare earth elements in place of Ca or Sr are of much interest because it leads to structural stability and helps in understanding the nature of charge carriers as well as the effect of variation of carrier concentration of the system [9–24]. Most of the substitution of rare earth elements are attempted on the Ca site [9–19] and a few in the Sr site [21,22]. Within the rare earths only a few studies have been made on Yb substitution for Ca [16–19]. In the solid state reaction method for Yb doping in $\text{Bi}_2\text{Sr}_2\text{Ca}_{1-x}\text{Yb}_x\text{Cu}_2\text{O}_y$, the maximum T_C is obtained for $x = 0.2-0.25$ [17,18].

* Corresponding author. Tel.: +91 471 2515373; fax: +91 471 2491712.
E-mail address: syam@csrrlrd.ren.nic.in (U. Syamaprasad).

For thick films prepared by partial melt technique T_C values depend primarily on the processing conditions which determine the solubility of Yb in the Bi-2212 matrix and amount of secondary phases. The highest T_C is obtained for the samples in which the amounts of secondary phases are minimized. The T_C decreases gradually when x in the thick films exceeds 0.25 [17]. Our recent studies on the addition of rare earth element Pr [23] on (Bi,Pb)-2212 leads to an enhancement of T_C as well as J_C . As a continuation of the above work, and to understand the effect of other rare earth substitution, in the present work, a systematic study on the addition of Yb on the superconducting properties of (Bi,Pb)-2212 was carried out.

2. Experimental

Yb added (Bi,Pb)-2212 superconductors were prepared by solid state synthesis with a general stoichiometry of $\text{Bi}_{1.7}\text{Pb}_{0.4}\text{Sr}_{2.0}\text{Ca}_{1.1}\text{Cu}_{2.1}\text{Yb}_x\text{O}_y$ (where $x = 0, 0.1, 0.2, 0.3, 0.4,$ and 0.5) using high purity chemicals $\text{Bi}_2\text{O}_3, \text{PbO}, \text{SrCO}_3, \text{CaCO}_3, \text{CuO}$ and Yb_2O_3 (Aldrich, >99.9%). Stoichiometric amounts of the ingredients were weighed using an electronic balance (Mettler AE 240), thoroughly mixed and ground using an agate mortar and pestle. The samples

are then calcined in air at different temperatures (800 °C/15 h, 820 °C/20 h, 840 °C/40 h) with a heating rate of 3 °C/min. Intermediate grinding was done between each stages of calcination. After calcination the samples were pelletised using a cylindrical die of 12 mm diameter under a force of 60 kN. The pellets are then heat treated at 845 °C for 100 h (50 + 50) in two stages with one intermediate pressing at the same force.

Phase analysis of the samples was done using XRD (Phillips X'pert Pro) employing X'celerator and monochromator at the diffracted beam side. Phase identification was performed using X'Pert High score software in support with ICDD-PDF 2 database. The densities of the pellets before and after the two stages of sintering were calculated by measuring the mass and dimensions of the pellets. The critical temperature and critical current were measured using four probe method with 1 μV/cm criterion using a Keithley nano voltmeter (model 181), a Keithley constant current source (model 220) and a Lakeshore Temperature controller (model 340). Microstructural examination of the samples was done using SEM (JEOL JSM 5000LV).

The samples will be hereafter denoted as Yb0, Yb1, Yb2, Yb3, Yb4, Yb5 with Yb content in $\text{Bi}_{1.7}\text{Pb}_{0.4}\text{Sr}_{2.0}\text{Ca}_{1.1}\text{Cu}_{2.1}\text{Yb}_x\text{O}_y$, where $x = 0, 0.1, 0.2, 0.3, 0.4, 0.5,$ respectively.

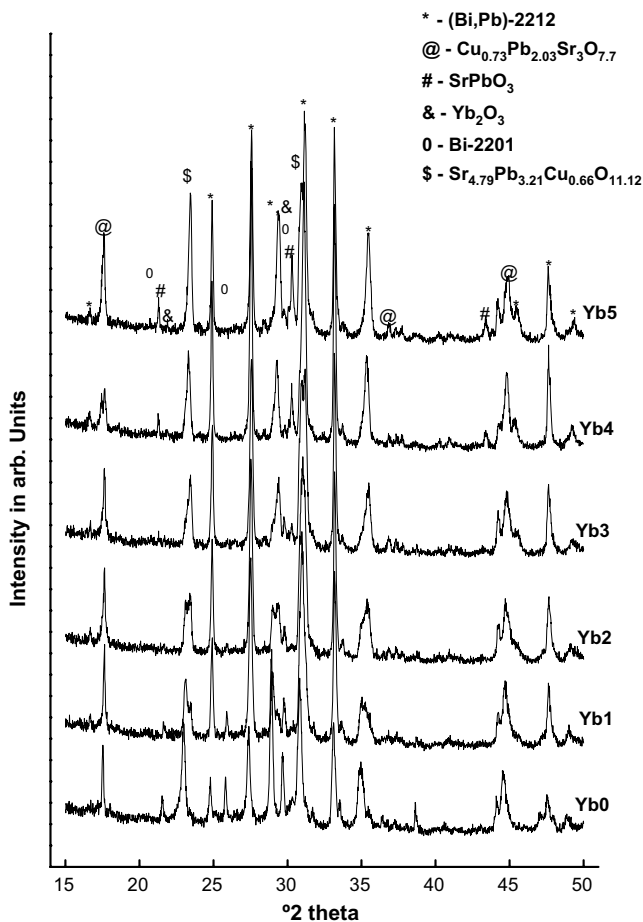


Fig. 1. X-ray diffraction patterns of the samples calcined at 820 °C/20 h.

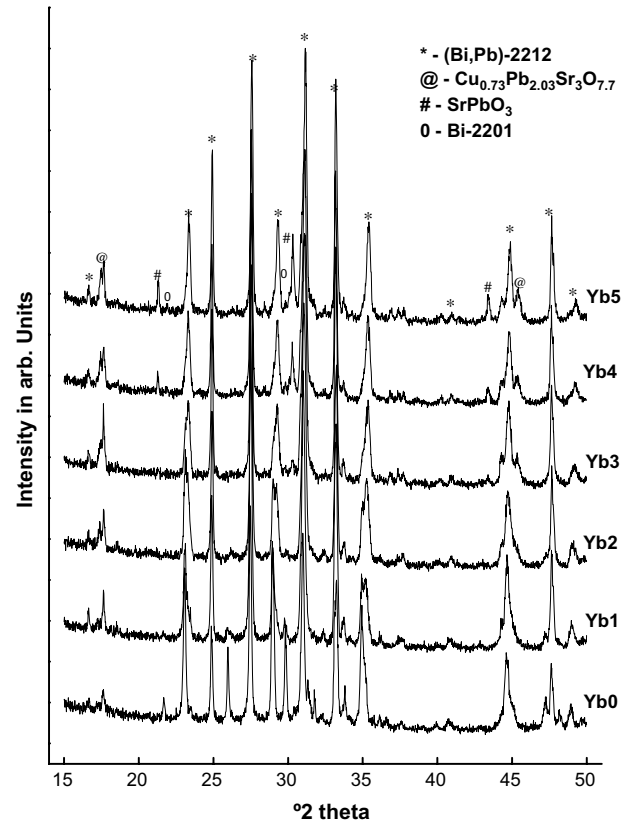


Fig. 2. X-ray diffraction patterns of the samples after calcination at 840 °C/40 h.

3. Results and discussion

Fig. 1 shows the XRD patterns of the samples after the calcination at 820 °C/20 h. The major phases detected are (Bi,Pb)-2212, Bi-2201, $\text{Cu}_{0.73}\text{Pb}_{2.03}\text{Sr}_3\text{O}_{7.7}$, SrPbO_3 , Yb_2O_3 and $\text{Sr}_{4.79}\text{Pb}_{3.21}\text{Cu}_{0.66}\text{O}_{11.12}$, as referred in the ICDD-PDF 2 data. Comparing the peak intensities, it can be seen that the volume fraction of Bi-2201 decreases and (Bi,Pb)-2212 increases with increasing Yb content. This shows that Yb addition favours the growth of formation of (Bi,Pb)-2212.

The XRD patterns of the samples after the calcination at 840 °C/40 h is shown in Fig. 2. At this stage very small percentage of Bi-2201 is present in Yb0 and Yb1. In the patterns of Yb4 and Yb5 peaks of SrPbO_3 is present. The major peaks present in all samples are that of (Bi,Pb)-2212 and very small fraction of $\text{Cu}_{0.73}\text{Pb}_{2.03}\text{Sr}_3\text{O}_{7.7}$ is present in all the samples.

Fig. 3 shows the XRD patterns of the samples after the last stage of sintering. The only phase detected in all the samples at this stage is (Bi,Pb)-2212 except for Yb4 and Yb5, where a small quantity of SrPbO_3 and $\text{Cu}_{0.73}\text{Pb}_{2.03}\text{Sr}_3\text{O}_{7.7}$ are also detected.

Fig. 4 shows the density variation of the samples after different stages of sintering as a function of Yb content. The density values as percentages of the theoretical density of (Bi,Pb)-2212 (6.6 g/cc) are shown on the right axis of the

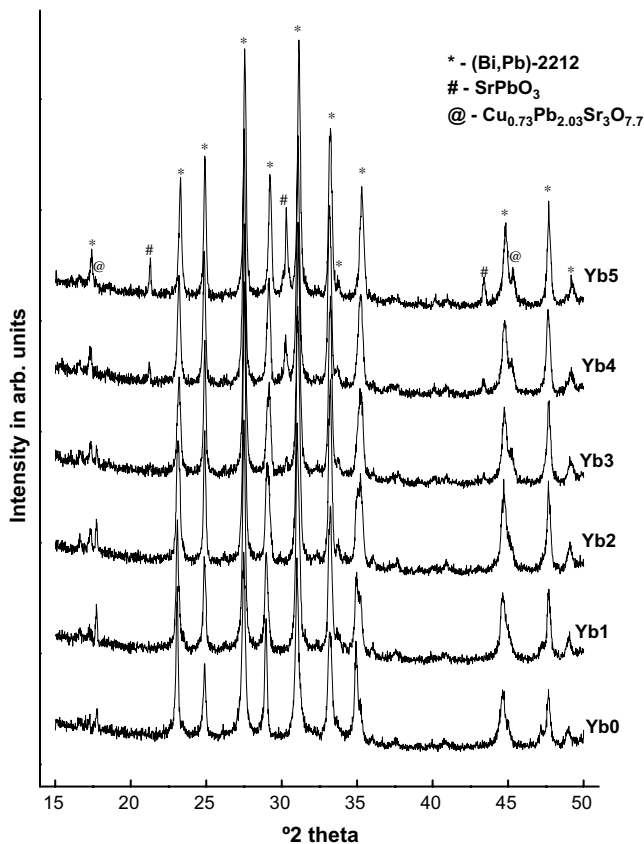


Fig. 3. X-ray diffraction patterns of the samples after last stage heat treatment.

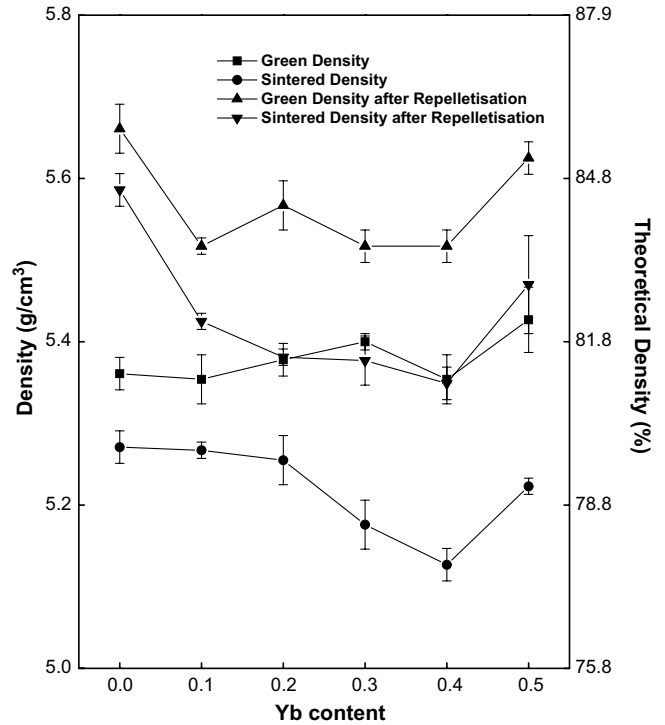


Fig. 4. Density variation of the samples after different stages of heat treatment.

figure. From the graph, it is clear that the sintered density of all the samples is less than the corresponding density prior to heat treatment. It is usually referred to as ‘retrograde densification’ and it is a characteristic property of BSCCO system. It is also noted that Yb5 sample shows an increase in density comparing with other Yb added samples.

The lattice parameter calculations were done by assuming orthorhombic symmetry for (Bi,Pb)-2212. The varia-

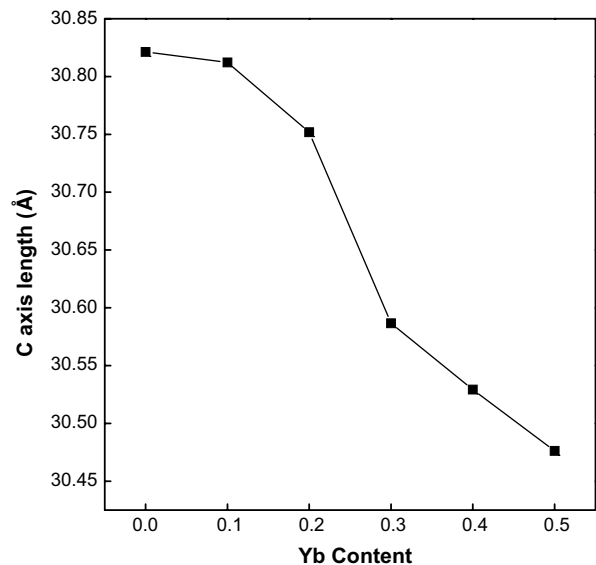


Fig. 5. Variation of *c*-axis parameter of the samples (after last stage heat treatment) as a function of Yb content.

tion of c -axis parameters of the samples after the last stage of sintering are shown in Fig. 5. It is observed that the c -axis contracts with increase of Yb content, but a - and b -axis have no considerable change.

The SEM micrographs of the samples after the last stage of sintering taken in the back scattered mode is shown in Fig. 6. The typical clean and flaky grain morphology of BSCCO is observed for Yb0 sample. But for Yb added samples grain size is smaller than Yb0 and it decreases with increase in Yb content. From Yb1 onwards a secondary phase having round edges are found distributed in the main matrix of the samples and for Yb5 sample colonies of secondary phases are seen which are separated from the main matrix. Fig. 6 also shows that the porosity of the sample increases as the Yb content increases. This may be the reason for the decrease in density of Yb added sample. The

small increase in density of Yb5 sample (Fig. 4) may due to the higher density of the secondary phase colonies.

Fig. 7 shows the variation of normalized resistivity as a function of temperature for different samples. All the samples show metallic behaviour above T_C . Yb added samples show much higher $T_{C-onset}$ than the pure sample. Yb2 sample shows the maximum $T_{C-onset}$ of 94.5 K whereas the pure sample (Yb0) shows the $T_{C-onset}$ of 79 K. Yb3 sample also shows almost similar value of 94 K. From Yb4 sample onwards T_C decreases. Fig. 8 shows the variation of $T_{C-onset}$ with Yb content. It shows that $T_{C-onset}$ reaches a maximum at Yb2 and then decreases. Table 1 gives the $T_{C-onset}$ and T_{C-zero} values of different samples.

The variation of critical current density (J_C) as a function of Yb content is shown in Fig. 9. Yb2 sample shows a J_C of 688 A/cm² at 64 K when the pure sample shows a

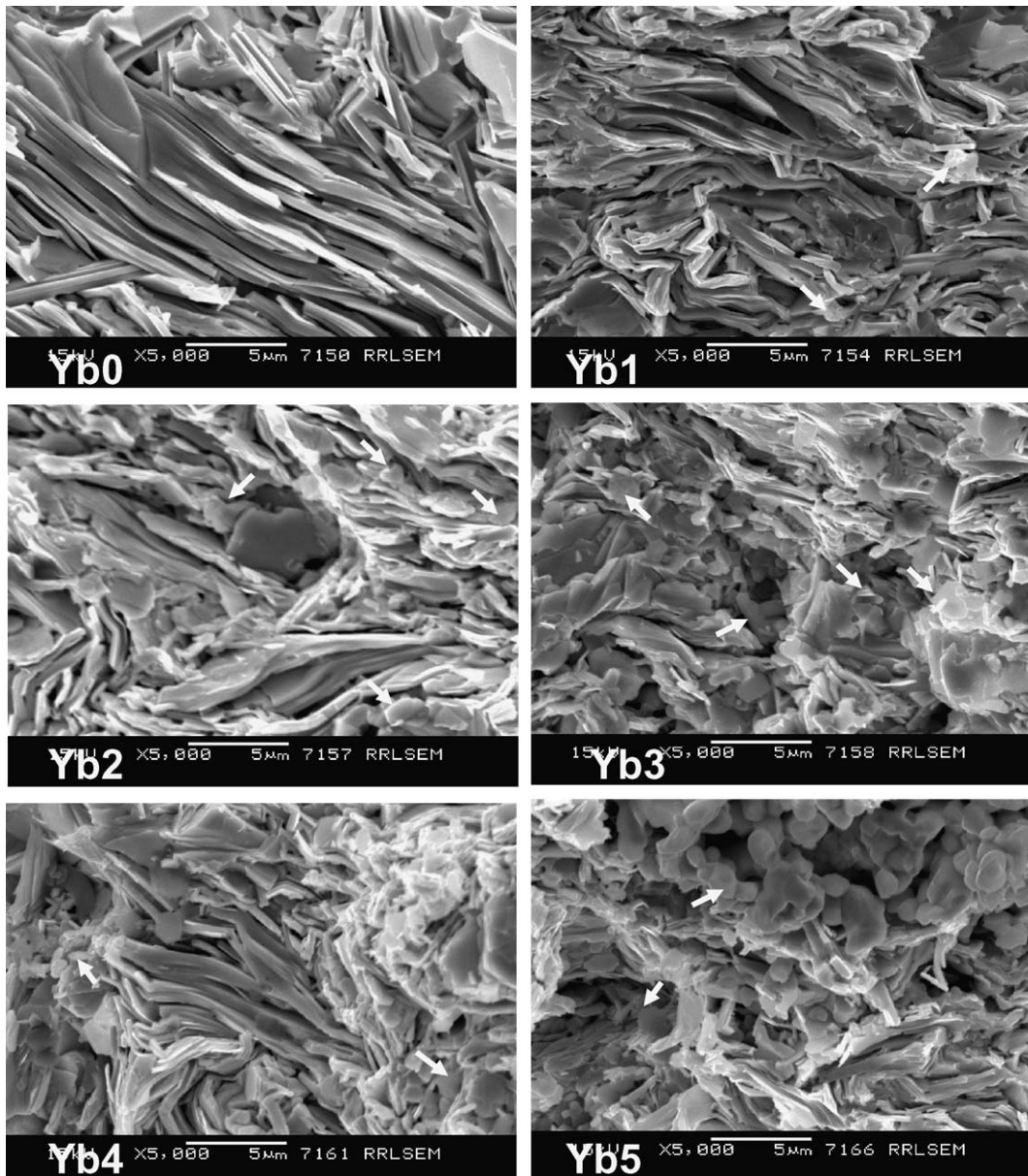


Fig. 6. SEM micrographs of the samples after last stage heat treatment, taken in back scattered mode (secondary phases are shown by arrows).

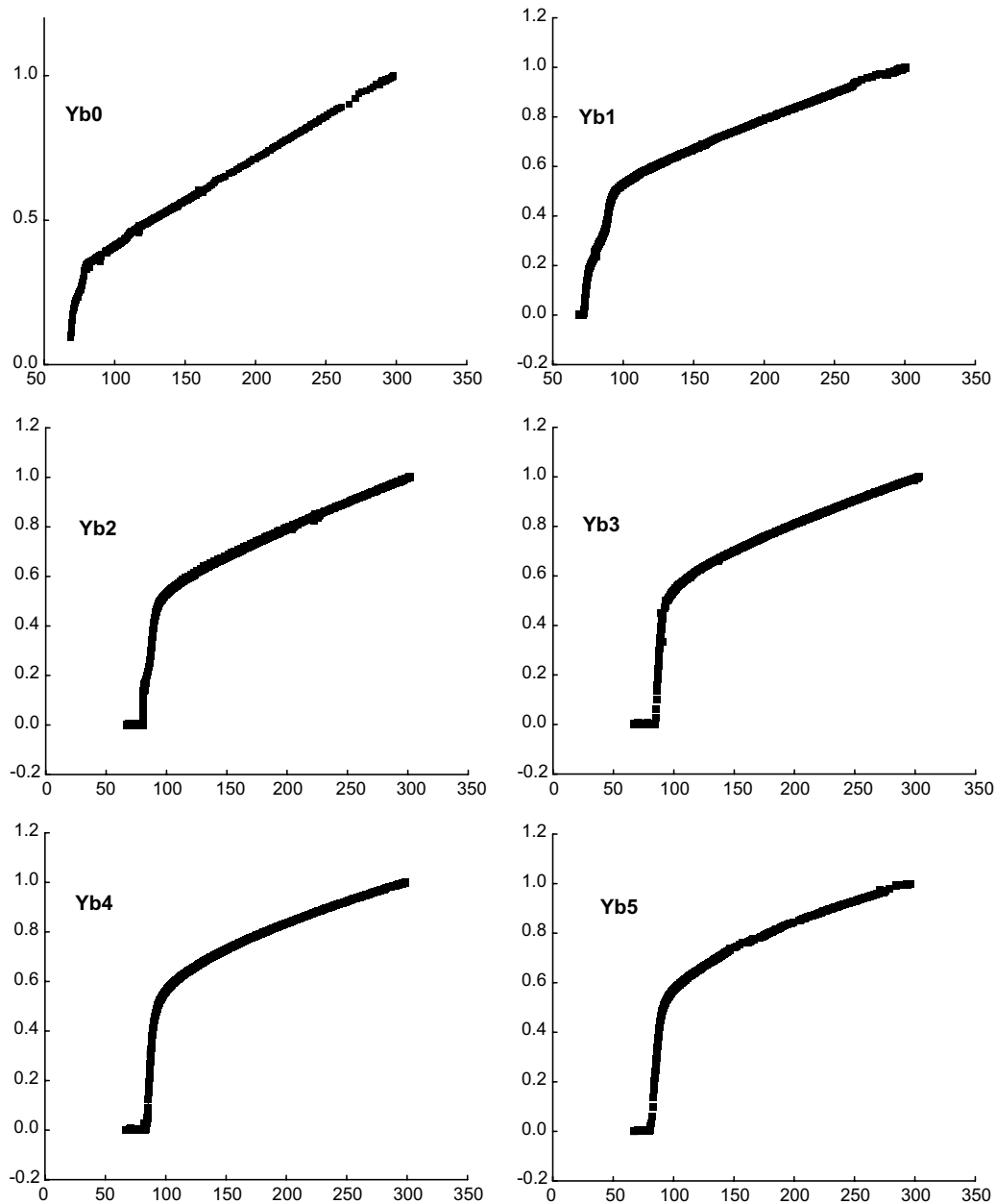


Fig. 7. Variation of the normalized resistivity of the samples as a function of temperature.

J_C of 110 A/cm². These results show that optimum addition of Yb ($x = 0.2$) highly enhances T_C as well as J_C of (Bi,Pb)-2212. These results are comparable with our earlier studies in the case of Pr [23]. There also J_C and $T_{C-onset}$ becomes maximum at $x = 0.2$ in the stoichiometry $\text{Bi}_{1.7}\text{Pb}_{0.4}\text{Sr}_{2.0}\text{Ca}_{1.1}\text{Cu}_{2.1}\text{Pr}_x\text{O}_y$.

With the increase of Yb content the c -axis value decreases and it implies that Yb occupies the crystal structure (Fig. 5). This decrease may be attributed to the fact that the addition of Yb leads to an increase in the oxygen content [1]. The excess oxygen could be incorporated into the Bi–O layers. This induces a contraction of Bi–O layers and causes an increase in the covalency of Bi–O bonds [24] which results in the decrease of the c -axis. The decrease in

c -axis length is slower after $x > 0.3$. This may be due to the saturation of excess oxygen in high doping level. Comparing the ionic radius of Yb^{3+} (1.008 Å) with that of Ca^{2+} (0.99 Å), Sr^{2+} (1.12 Å) and Bi^{3+} (0.96 Å), Yb^{3+} ions may be substituted to any of the three cations. But the XRD patterns of the samples after the last stage heat treatment show the presence of SrPbO_3 along with the peaks of (Bi,Pb)-2212 and $\text{Cu}_{0.7}\text{Pb}_{2.03}\text{Sr}_3\text{O}_{7.7}$, which shows that Sr^{2+} ions are replaced by the Yb^{3+} ions and forms the secondary phase SrPbO_3 . In the case of Pr addition no such secondary phases were detected in the XRD [23], but EDX gave the evidences of a secondary phase. The SEM pictures give the evidence of these secondary phases. At overdoped conditions the excess Yb ions form the second-

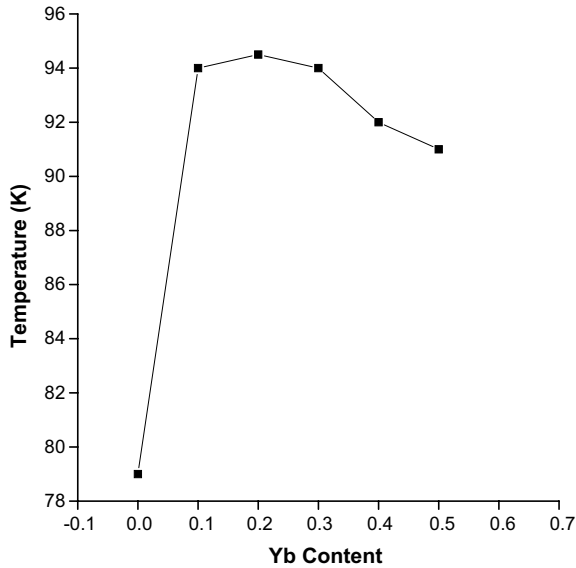


Fig. 8. Variation of $T_{C\text{-onset}}$ as a function of Yb content.

Table 1
 $T_{C\text{-zero}}$ and $T_{C\text{-onset}}$ values of the samples

Sample name	$T_{C\text{-zero}}$ (K)	$T_{C\text{-onset}}$ (K)
Yb0	67.5	79
Yb1	72	94
Yb2	81.5	94.5
Yb3	85	94
Yb4	83	92
Yb5	80	91

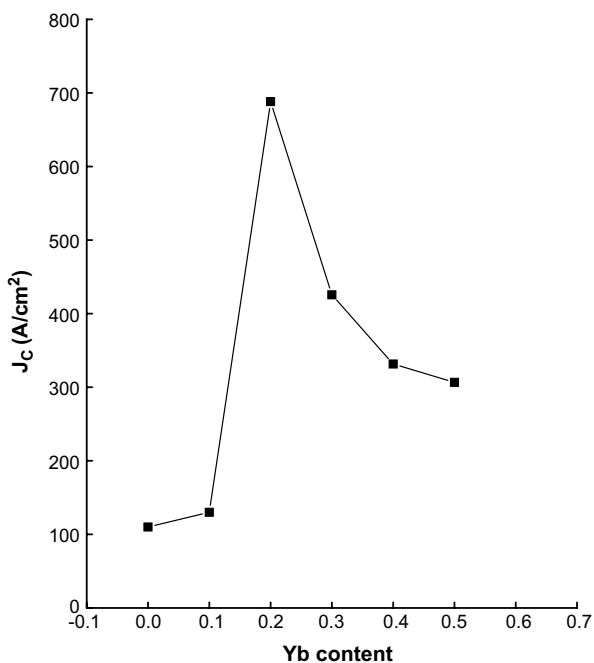


Fig. 9. Variation of J_C as a function of Yb content.

ary phase colonies which are visible in the SEM of Yb5 sample. Also one of the reasons for the decrease in the c -parameter may be due to the smaller ionic size of Yb^{3+} ion compared to the Sr^{2+} ion.

The above results show that the addition of Yb in (Bi,Pb)-2212 replaces the Sr^{2+} ions by Yb^{3+} ions. This replacement of divalent cation by a trivalent ion will cause changes in the carrier concentration and can lead to inhomogeneities of the charge reservoir layers. Doping in the charge reservoir layers may be required to achieve the desired carrier concentration, defects in or near CuO layers are detrimental to superconducting properties such as J_C and T_C . Buzea and Yamashita [25] gives a theoretical explanation that the T_C variation with doping concentration (x) depends on the ratio of superconducting volume and total volume and becomes maximum at a particular value of x , and then decreases.

4. Conclusions

Phase evolution, microstructure and superconducting properties of (Bi,Pb)-2212 due to Yb addition have been studied. It was found that Yb improves (Bi,Pb)-2212 formation, also the critical current density (J_C) and critical temperature (T_C) of (Bi,Pb)-2212 can be increased by the addition of Yb. J_C (688 A/cm²) and $T_{C\text{-onset}}$ (94.5 K) becomes maximum when $x = 0.2$ in the stoichiometry $\text{Bi}_{1.7}\text{Pb}_{0.4}\text{Sr}_{2.0}\text{Ca}_{1.1}\text{Cu}_{2.1}\text{Yb}_x\text{O}_y$. This is due to the charge carrier concentration as a result of the substitution of Sr^{2+} ions by Yb^{3+} ions. The decrease of J_C and T_C after $x > 0.2$ is due to the formation of secondary phase produced after the saturation of Yb^{3+} in the Sr^{2+} site. This Sr containing secondary phase is detected in the XRD analysis of the Yb added samples and the secondary phase colonies seen in the SEM of Yb5 may be this Sr containing phase.

Acknowledgement

The author A. Biju acknowledges University Grants Commission for granting FIP fellowship.

References

- [1] J.M. Tarascon, P. Barboux, G.W. Hull, R. Ramesh, L.H. Greene, M. Grioud, M.S. Hedge, W.R. McKinnon, Phys. Rev. B 38 (1989) 4316.
- [2] K. Koyama, S. Kanno, S. Noyuchi, Jpn. J. Appl. Phys. 29 (1990) L53.
- [3] Y. Li, S. Kaviraj, A. Berenov, G.K. Perkins, J. Driscoll, A.D. Caplin, G.H. Cao, Q.Z. Ma, B. Wang, L. Wei, Z.X. Chao, Physica C 355 (2001) 51.
- [4] H. Fujii, Y. Hishinuma, H. Kitaguchi, H. Kumakura, K. Togano, Physica C 331 (2000) 79.
- [5] T. Motohashi, Y. Nakayama, T. Fujita, K. Kitazawa, J. Shimoyama, K. Kishio, Phys. Rev. B 59 (1999) 14080.
- [6] J. Shimoyama, Y. Nakayama, K. Kitazawa, K. Kishio, Z. Hiroi, I. Chong, M. Takano, Physica C 281 (1997) 69.
- [7] W.D. Wu, A. Keren, L.P. Le, B.J. Sternlieb, G.M. Luke, Y.J. Uemura, Phys. Rev. B 47 (1993) 8172.

- [8] I. Chong, M. Hiroi, J. Izumi, Y. Shimoyama, Y. Nakayama, K. Kishio, T. Terashima, Y. Bando, M. Takano, *Science* 276 (1997) 770.
- [9] C.A.M. dos Santos, S. Moehlecke, Y. Kopelevich, A.J.S. Machado, *Physica C* 390 (2003) 21.
- [10] X.G. Lu, X. Zhao, X.J. Fan, X.F. Sun, W.B. Wu, H. Zhang, *Appl. Phys. Lett.* 76 (2000) 3088.
- [11] H. Jin, J. Kotzler, *Physica C* 325 (1999) 153.
- [12] V.P.S. Awana, S.K. Agarwal, R. Ray, S. Guptha, A.V. Narlikar, *Physica C* 43 (1992) 1991.
- [13] A. Sattar, J.P. Srivastava, S.V. Sharma, T.K. Nath, *Physica C* 266 (1996) 335.
- [14] V.P.S. Awana, L. Menon, S.K. Malik, *Phys. Rev. B* 51 (1995) 9379.
- [15] C.A.M. dos Santos, G.S. Pinto, B. Ferreira, A.J.S. Machado, *Physica C* 354 (2001) 388.
- [16] A.Y. Ilyushechkin, T. Yamashita, L. Boskovic, I.D.R. Mackinnon, *Supercond. Sci. Technol.* 17 (2004) 1201.
- [17] R. Somasundaram, R. Vijayaraghavan, R. Nagarajan, R. Seshadri, A.M. Umarji, C.N.R. Rao, *Appl. Phys. Lett.* 56 (1990) 487.
- [18] R. Yoshizaki, J. Fujikami, M. Akamatsu, H. Ikeda, *Supercond. Sci. Technol.* 4 (1991) S421.
- [19] M.J. Casanove, P. Baules, E. Snoeck, C. Roucau, *Physica C* 159 (1989) 461.
- [20] P. Sumana Prabu, M.S. Ramachandra, U.V. Varadaraju, G.V. Subbha Rao, *Phys. Rev. B* 50 (1994) 6929.
- [21] H. Fuji, H. Kumakura, K. Togano, *Physica C* 355 (2001) 111.
- [22] P. Murugakoothan, R. Jayavel, S.R. Venkatswara Rao, et al., *Supercond. Sci. Technol.* 7 (1994) 367.
- [23] R.P. Aloysius, P. Guruswamy, U. Syamaprasad, *Supercond. Sci. Technol.* 18 (2005) L1.
- [24] C.C. Torardi, J.B. Parise, M.A. Subramanian, J. Gopalakrishnan, A.W. Sleight, *Physica C* 157 (1989) 115.
- [25] C. Buzea, T. Yamashita, *Physica C* 357–360 (2001) 288.